



## Carbon Monoliths: A Comparison with Granular Materials

BARRY CRITTENDEN\*, ANDREW PATTON, CHRISTOPHE JOUIN AND SEMALI PERERA

*Department of Chemical Engineering, University of Bath, Bath, BA2 7AY, UK*

b.d.crittenden@bath.ac.uk

STEVE TENNISON

*MAST Carbon Ltd, Henley Park, Guildford, Surrey, GU3 2AF, UK*

JUAN ANGEL BOTAS ECHEVARRIA

*Department of Chemical, Environmental and Materials Technology, Universidad Rey Juan Carlos, Móstoles, Madrid, Spain*

**Abstract.** An activated carbon monolith synthesized from a phenolic resin precursor provides capacity and kinetic properties which compare most favourably with the same mass of its granular counterpart. Experimental data have been obtained using a dynamic, flow apparatus. The comparative performances are readily explained by an analysis of internal and external mass transfer coefficients. The effect of axial dispersion is neglected. Internal mass transfer coefficients are based on the linear driving force assumption, being approximated for the monolith by a geometric transformation from the square channel to a hollow cylinder impervious to mass at its outer radius. The monolith is predicted to have a pressure drop which is less than 6% of that of its equivalent granular system.

**Keywords:** monoliths, activated carbon, volatile organic compounds, linear driving force

### 1. Introduction

Monoliths comprise bundles of channels in a solid that resembles a honeycomb structure. Whilst the regular hexagon is good in terms of mass transfer and pressure drop properties (Patton et al., 2004), the commonest channel is square since this is simplest to form. Activated carbon monoliths have been used to adsorb volatile organic compounds (Gadkaree, 1998; Yates et al., 2000; Tennison et al., 2001; Fuertes et al., 2003; Valdés-Solís et al., 2003a). Free of binder, they are manufactured commercially (MAST Carbon Ltd, UK) by carbonising and then activating extruded phenolic resins. This manufacturing route provides for a unique, detailed control over the pore structure at the cell, micropore and macropore levels. The monoliths are also electrically conducting, thereby facilitating rapid ther-

mal swing operation at low voltage difference, providing the opportunity to reduce equipment size and adsorbent inventories in VOC recovery systems (Tennison et al., 2001). Of the external parameters, the channel dimension,  $a$ , wall thickness,  $t_w$ , and the cell shape, need to be optimised for high kinetic performance balanced against low pressure drop, especially for VOC recovery applications (Patton et al., 2004). With the flexibility afforded by the independent geometric parameters,  $a$  and  $t_w$ , the opportunity exists to tailor or optimise the design for particular applications. Flexibility is much more limited with granular materials.

### 2. Materials and Experimental Method

The adsorption of  $n$ -butane from air was used to compare activated carbon in monolithic and granular forms. The MAST Carbon square channel monolith had a

\*To whom correspondence should be addressed.

cell density of  $\approx 89$  cells/cm<sup>2</sup> with  $a = 0.63$  mm and  $t_w = 0.43$  mm. Surfaces were rough and somewhat irregular in shape (Fig. 1). Granules, of size range 600–1400  $\mu$ m, were obtained by crushing samples of the monolith. Hence, the internal structures of the granules and monolith were identical. Surface and pore properties were obtained by nitrogen adsorption (Micromeritics ASAP 2010). BET and Langmuir surface areas were 806 and 1051 m<sup>2</sup>/g, respectively. Total pore and micropore volumes were 0.371 cm<sup>3</sup>/g, and the pore radius was  $\approx 0.41$  nm (Botas Echevarria et al., 2003). The materials have no mesopore structure and the macropore diameters are  $\approx 5$   $\mu$ m (Tennison, 1998).

Dynamic experiments were carried out in a flow apparatus (Botas Echevarria et al., 2003). The adsorption column contained 26.11 g of adsorbent, whether monolith or granules. The monolith length and diameter were 94.1 and 20.4 mm, respectively, whilst the granular bed length and diameter were 122.0 and 21.2 mm, respectively. The total gas flow rate was fixed at 1 or 3 litres/min at 40°C and the concentration of *n*-butane was fixed at 3 or 7% in nitrogen. The feed concentration and progress of the breakthrough curve were monitored continuously using a flame ionisation detector. The temperature of gas leaving the adsorbent was monitored by a thermocouple. Prior to all experiments, the adsorbent was regenerated for four hours under a nitrogen flow of 1 litre/min at 400°C. The adsorption experiments were terminated after full breakthrough had occurred.

### 3. Results

A summary of the results is given in Table 1. Both the breakthrough time and the loading at the point of breakthrough for the two forms of carbon were found to be more or less equal. The design of the monolith was intended to give this result. A comparison of Figs. 2 and 3, showing the effect of flow rate, reveals that whilst the

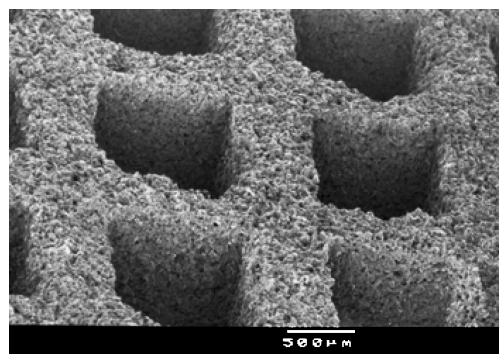


Figure 1. Scanning electron micrograph of MAST Carbon monolith (Patton et al., 2004).

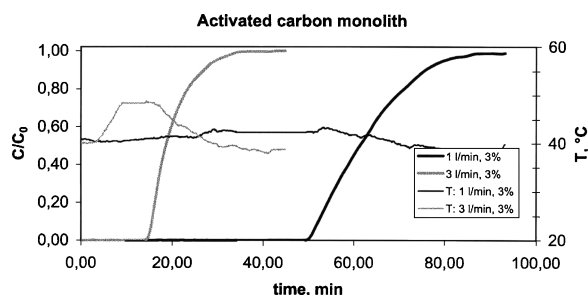


Figure 2. Breakthrough curves and temperature profiles for the monolith.

final portion of the monolith breakthrough curve was quite different from that for the granules, the initial portions of the curves were quite similar. A similar observation was made for the breakthrough curves as a function of feed concentration.

Table 1 shows that the loading after breakthrough decreases with increasing butane concentration for both forms of the adsorbent. The cause of this apparent anomaly is the progress through the column of a larger exotherm at the higher concentration which, in turn, causes a reduction in equilibrium loading. This effect has been observed in other dynamic adsorption column experiments (Crittenden and Ben-Shebal, 1992).

Table 1. Summary of column performance.

Flow rate (litres/min)	Butane conc (%)	Bed of granules			Monolith		
		Breakthrough time (mins)	Loading at breakthrough (%)	Loading after breakthrough (%)	Breakthrough time (mins)	Loading at breakthrough (%)	Loading after breakthrough (%)
1	3	46	13.47	16.56	50	14.43	18.55
1	7	15	10.77	13.14	15	10.49	14.10
3	3	14	12.82	16.59	14	12.34	17.72

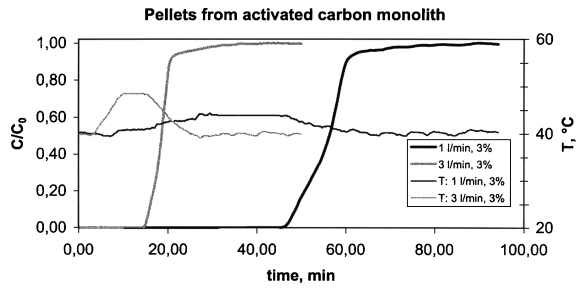


Figure 3. Breakthrough curves and temperature profiles for the granules.

Table 1 shows, as expected, that the loadings after breakthrough were quite similar for all four experiments in which the feed concentration was maintained at the lower value of 3%, but the flow rate was varied.

#### 4. Analysis and Design

Approximate HETP solutions to adsorption in rectangular coated chromatography columns are provided by Golay (1958, 1981) and Spangler (1998). Shah et al. (1996) obtained numerical solutions for a monolithic adsorbent when mass transfer was microporous diffusion controlled but failed to obtain a solution when the macropore diffusion resistance became important. Valdés-Solís et al. (2003b) developed a numerical model for the adsorption of VOCs to find that it was necessary to assume a parabolic velocity distribution in the carbon-ceramic monolith. Crittenden et al. (2001) analysed the channel and internal mass transfer effects to determine the dimensions of a square channel zeolitic monolith which would have a comparative kinetic performance to an equivalent bed of pellets. In the present study on carbons, the similarity in the breakthrough times for the two adsorbent forms is also explained in terms of their internal and external mass transfer coefficients (Patton et al., 2004). The Ranz and Marshall (1952) correlation for the Sherwood number,  $Sh$ , is used to obtain the external (film) mass transfer coefficient,  $k$ , for a packed bed in which axial dispersion is not significant and for Schmidt numbers,  $Sc$ , up to 160:

$$Sh = \frac{k d_p}{D} = 2 + 0.6 Sc^{1/3} Re_p^{1/2} \quad (1)$$

The exact value of the molecular diffusion coefficient,  $D$ , for a VOC in nitrogen is not essen-

tial for the comparison; the value is typically of the order of  $10^{-5}$  m<sup>2</sup>/s (Janssen and Warmoeskerken, 1987). The viscosity and density at 40°C are  $1.92 \times 10^{-5}$  Ns/m<sup>2</sup> and 1.127 kg/m<sup>3</sup>, respectively (Janssen and Warmoeskerken, 1987). Hence,  $Sc \approx 1.7$ . The particle diameter,  $d_p$ , is taken to be 1.0 mm and the voidage,  $e$ , to be 0.4. For flow rates of 1 and 3 litres/min, the corresponding values of Reynolds number,  $Re_p$ , are 7.3 and 21.8. Hence the external film mass transfer coefficients are 0.039 and 0.053 m/s, respectively.

Setting aside the debate over the selection of a correlation for the square channel Sherwood number (Valdés-Solís et al., 2003; Patton et al., 2004), the Hawthorn (1974) semi-analytical equation is used to obtain the asymptotic value of the external mass transfer coefficient for the monolith:

$$Sh = \frac{k d_{ch}}{D} = 2.98 \left( 1 + 0.095 Re_m Sc \frac{d_{ch}}{L} \right)^{0.45} \quad (2)$$

The channel dimension,  $d_{ch}$ , is the hydraulic mean diameter which is equal to  $a$ , the length of the side of the square channel. The asymptotic mass transfer coefficient is given by:

$$k = 2.98 D / a \quad (3)$$

Hence the asymptotic mass transfer coefficient for the monolith is equal to 0.047 m/s. This value is unaffected by the flow rate down the channel, provided that flow is laminar.  $Re_m = 16$  for a total flow rate of 3 litres/min. The external mass transfer coefficient for the granules at the higher flow rate is 13% greater than that for the monolith, whilst for the lower flow rate it is 17% lower. It can be seen, correspondingly, from Table 1, that the loading at breakthrough for the bed of granules is marginally better than that for the monolith at the higher flow rate, whilst the converse is the case for the lower flow rate. At the lower flow rate, the breakthrough time is, correspondingly, shorter for the bed of granules. It is clear, therefore, that the monolith has been designed to compare favourably with the bed of granules at least in terms of external mass transfer coefficient.

The linear driving force approximation is used only as an approximation to provide an initial and approximate comparison of the rates of adsorption,  $d\bar{q}/dt$ , (Glueckauf, 1955; Glueckauf and Coates, 1947).  $q^*$  and  $\bar{q}$  are the equilibrium and average loadings. For rigorous design and analysis, caution needs to be taken

if the isotherm is highly favourable (Ruthven, 1984) which is the case for the MAST Carbon materials. For spherical particles:

$$\frac{d\bar{q}}{dt} = \frac{60De}{d_p^2}(q^* - \bar{q}) \quad (4)$$

The effective diffusion coefficient,  $D_e$ , is the same for the granules and monolith and need not be evaluated. For 1 mm diameter particles, the value of  $60/d_p^2$  is equal to  $6.0 \times 10^7$ . A linear driving force expression for a square channel monolith has been derived by Patton et al. (2004). It is based on the assumption that a square channel of inner dimension,  $a$ , and wall thickness,  $t_w$ , can be transformed to a cylindrical channel of inner radius  $r_i$  and outer radius  $r_o$  which is impervious to mass transfer on its outer surface. The geometry transformation is based on the cylindrical channel having the same surface area and wall volume per unit length as the square channel. The geometry transformations are:

$$r_i = \frac{2a}{\pi} \quad (5)$$

$$r_o = \sqrt{\frac{4t}{\pi}(t + a) + r_i^2} \quad (6)$$

Using the quadratic driving force approximation (Liaw et al., 1979), Patton et al. (2004) derived the linear driving force expression for the equivalent hollow cylinder:

$$\frac{d\bar{q}}{dt} = \frac{4D_e(q^* - \bar{q})}{\left[\left(\frac{r_o}{r_i} - 1\right)(r_o^2 - r_i^2) - \frac{1}{r_i(r_o - r_i)}\left(\frac{1}{2}(r_o^4 - r_i^4) - \frac{4r_o}{3}(r_o^3 - r_i^3) + r_o^2(r_o^2 - r_i^2)\right)\right]} \quad (7)$$

With  $t = t_w/2$  in this equation, it can be shown that for the monolith:

$$\frac{d\bar{q}}{dt} = 4.4 \times 10^7 De(q^* - \bar{q}) \quad (8)$$

The coefficient in the linear driving force expression for the monolith is 27% less than that calculated for the bed of granules. The comparison is especially favourable bearing in mind the potential errors involved. Firstly Eq. (4) is used for particles which not only are somewhat irregular in shape (having been made by crushing and grinding monolith pieces) but which also have a range of sizes (with a median of 1 mm). Secondly, the validity of the geometry transformation for the monolith has not been evaluated ex-

perimentally. Thirdly, the monolith channels are not smooth, straight or uniform in dimension (Fig. 1). When both the external and internal coefficients are compared for the two shapes of activated carbon, it is not surprising that the dynamic performances, particularly for the 3 litres/min feed flow rate, are almost the same. It is more-or-less confirmed that, for this particular application involving the adsorption of a dilute hydrocarbon from air, the monolith geometry competes very well with the equivalent bed of granules on both experimental and theoretical grounds.

It can be seen from Eq. (2) that the external mass transfer performance of a monolith can be improved by reducing the channel size. For the simplest form of monolith device, namely the parallel plate contactor, Ruthven and Thaeon (1996) were able to show that a substantial advantage in terms of reduced pressure drop was available for a given number of theoretical stages in an adsorption column. Additionally, the HETP could be reduced by reducing the spacing between the adsorbent surfaces. It can be seen from Eqs. (5)–(7) that the internal mass transfer performance can be improved by reducing the wall thickness. Hence, the challenge is to make thin walled monoliths with high cell densities.

The Ergun (1952) equation (in which  $u$  is the superficial velocity,  $L$  is the length of adsorbent,  $\mu$  is the viscosity and  $\rho$  is the density) can be used to show that the pressure drop,  $\Delta P$ , through the granules is 982 Pa at 3 litres/min:

$$\frac{\Delta P}{L} = 150 \frac{(1 - e)^2}{e^3} \frac{\mu u}{d_p^2} + 1.75 \frac{(1 - e)}{e^3} \frac{\rho u^2}{d_p} \quad (9)$$

The pressure drop along the monolith channel is given by Patton et al. (2004):

$$\frac{\Delta P}{L} = \frac{28.4 Q \mu}{a^4} \quad (10)$$

$Q$  is the volumetric flow rate through a channel.  $\Delta P$  at 3 litres/min is 56 Pa, that is, less than 6% of that for the equivalent bed of granules. The channel roughness should not affect the pressure drop since flow is laminar.

## 5. Conclusion

It has been demonstrated that it is possible to manufacture an activated carbon monolith that has a capacity

and dynamic mass transfer performance equal to that of the equivalent bed (same mass) of granules. The pressure drop however, is expected to be less than 6% of that for the bed of granules.

## References

- Botas Echevarria, J.A., S. Perera, and B.D. Crittenden, "Monolithic Adsorbents: A Comparison with Their Particulate Counterparts," in *Proc. 4th European Congress of Chemical Engineering*, Granada, Topic 7 abstracts, 2003.
- Crittenden, B.D. and S. Ben-Shehal, "Effect of Thermal Gradients on the Adsorptive Drying of Solvents in Packed Beds of Zeolite," *ICHEME Symposium Series*, **129**, 1147–1154 (1992).
- Crittenden, B.D., S. Perera, L.Y. Lee, and A. Gómez Crespo, "Monolithic Adsorbents in Environmental Protection," in *Proc 9th Int. Summer School on Chemical Engineering*, Ts. Sapunzhiev (Ed.), pp. 246–267, Bulgarian Academy of Sciences, Sofia, 2001.
- Ergun, S., "Fluid Flow through Packed Columns," *Chem. Eng. Progress*, **48**(2), 89–94 (1952).
- Fuertes, A.B., G. Marbán, and D.M. Nevskaya, "Adsorption of Volatile Organic Compounds by Means of Activated Carbon Fibre Monoliths," *Carbon*, **41**, 87–96 (2003).
- Gadkaree, K.P., "Carbon Honeycomb Structures for Adsorption Applications," *Carbon*, **36**, 981–989 (1998).
- Glueckauf, E., "Theory of Chromatography, Part 10: Formulae for Diffusion into Spheres and their Application to Chromatography," *Trans. Faraday Society*, **51**, 1540–1551 (1955).
- Glueckauf, E. and J.I. Coates, "Theory of Chromatography, Part IV: The Influence of Incomplete Equilibrium on the Front Boundary of Chromatograms and on the Effectiveness of Separation," *J. Chem. Soc.*, 1315–1321 (1947).
- Golay, M.J.E., "Theory of Chromatography in Open and Coated Tubular Columns with Round and Rectangular Cross-sections," *Gas Chromatography*, D.H. Desty (Ed.), pp. 36–55, Academic Press, New York, 1958.
- Golay, M.J.E., "The Height Equivalent to a Theoretical Plate of Retentionless Rectangular Tubes," *J. Chromatography*, **A216**, 1–8 (1981).
- Hawthorn, R.D., "Afterburner Catalysts—Effects of Heat and Mass Transfer between Gas and Catalyst Surface," *AIChE Symposium Series*, **70**, 428–438 (1974).
- Janssen, L.P.B.M. and M.M.C.G. Warmoeskerken, *Transport Phenomena Data Companion*, Edward Arnold, London, 1987.
- Liaw, C.H., J.S.P. Wang, R.A. Greenkorn, and K.C. Chao, "Kinetics of Fixed Bed Adsorption: A New Solution," *AIChEJ*, **25**, 376–381 (1979).
- Patton, A., B.D. Crittenden, and S.P. Perera, "Use of the Linear Driving Force Approximation to Guide the Design of Monolithic Adsorbents," *Trans IChemE*, **82A**, in press, 2004.
- Ranz, W.E. and W.E. Marshall, "Evaporation from Drops, Part II," *Chem. Eng. Progress*, **48**(4), 173–180 (1952).
- Ruthven, D.M., *Principles of Adsorption and Adsorption Phenomena*, p. 261, John Wiley & Sons, New York, 1984.
- Ruthven, D. M. and C. Thaeron, "Performance of a Parallel Passage Adsorbent Contactor," *Gas Sep. and Purif.*, **10**, 63–73 (1996).
- Shah, D.B., S.P. Perera, and B.D. Crittenden, "Adsorption Dynamics in a Monolithic Adsorber," *Fundam. of Adsorption*, M.D. LeVan (Ed.), pp. 813–820, Kluwer Academic Publishers, Boston, 1996.
- Spangler, G.E., Height Equivalent to a Theoretical Plate Theory for Rectangular GC Columns," *Anal. Chem.*, **70**, 4805–4816 (1998).
- Tennison, S.R., Phenolic Resin-Derived Activated Carbons, *Applied Catalysis A*, **173**, 289–311 (1998).
- Tennison, S.R., A. Blackburn, A. Rawlinson, R. Place, B.D. Crittenden, and S. Fair, "Electrically Regenerable Monolithic Adsorption System for the Recovery and Recycle of Solvent Vapours," in *Proc. AIChE Spring Meeting*, Manuscript 109e (2001).
- Valdés-Solís, T., M.J.G. Linders, F. Kapteijn, G. Marbán, and A.B. Fuertes, "Adsorption Performance of Carbon-Ceramic Monoliths at Low Concentration VOC," *Proc. of Carbon Conference*, Oviedo, p. 102, 2003a.
- Valdés-Solís, T., M.J.G. Linders, F. Kapteijn, G. Marbán, and A.B. Fuertes, "Modelling of the Breakthrough Performance of Carbon-Ceramic Monoliths in Gas Adsorption," *Proc. of Carbon Conference*, Oviedo, p. 166 (2003b).
- Yates, M., J. Blanco, P. Avila, and M.P. Martin, "Honeycomb Monoliths of Activated Carbon for Effluent Gas Purification," *Microporous and Mesoporous Materials*, **37**, 201–208 (2000).